PERGAMON

International Journal of Solids and Structures 37 (2000) 1955–1973

INTERNATIONAL JOURNAL OF SOLIDS and STRUCTURES

www.elsevier.com/locate/ijsolstr

On the lateral collapse of an identical pair of cylinders

A. Abdul-Latif*

ERBEM/GIM, IUT de Tremblay, Université Paris 8, 93290 Tremblay-en-France, France

Received 8 April 1997; in revised form 3 August 1998

Abstract

Superplastic tin–lead alloy, which has a sensitivity to strain rate in the range of (10^{-5}/s–10^{-3}/s), serves as a representative material to simulate the dynamic lateral collapse of an identical pair of hollow cylinders made from a classical engineering material as an energy dissipative system. Actual superplastic cylinders of various inside/outside diameter ratios ($R = d_i/d_o$) ranging from 0–0.473 are tested under different strain rates ($\dot{\varepsilon}$) varying from 10^{-5}/s–10^{-3}/s. The capacity of this system to absorb energy is governed by certain parameters. These parameters are the amount of the plastic strain and its rate, and the geometry of the employed cylinders. To understand the mechanism of deformation of this system at different strain rates, a successful trail is developed using different plasticine colored layers in the form of cylinders. A simple mathematical model is proposed to describe the mechanical behavior of these structures, simulating the dynamic lateral compression of rate-sensitive metallic cylinders as related to their use in an energy absorbing device. Predicted responses are in good agreement with experimental results.

Keywords: Lateral collapse; Energy dissipative system; Superplasticity; Strain rate; Strain rate sensitivity

1. Introduction

Energy dissipating devices are important in mitigating the damage and thus improving crashworthiness and vehicular collisions. A number of literature surveys representing the state of the art in this field (e.g., Ezra and Fay, 1972; Rawlings, 1974; Johnson and Reid, 1978, 1986; Jones, 1989) give detailed discussion of those techniques and theoretical treatments of different energy absorbing devices. These mechanical devices and elements that can be used in a wide variety of engineering applications depend upon the plastic deformation. Generally, the common structural elements are wires, bars, frames and tubes. Because of the widespread use of the tubular components in these devices, a focusing is done here on such elements. They can be plastically flattened due to lateral compression and can be laterally

* Corresponding author. Tel.: +33-1-4151-1224; fax: +33-1-4861-3874.
E-mail address: aabdul@europost.org (A. Abdul-Latif).

0020-7683/00/$ - see front matter
PII: S0020-7683(98)00335-7

crushed under local loads. Under axial compressive loadings, these elements can be also axi-symmetrically buckled. A great deal of attention has been given to the study of energy absorption. Recently, axial crushing of circular and square or rectangular sectioned tubes under static and dynamic loading conditions was conducted by many research programs and was reviewed by Abramowicz and Jones (1986), Jones (1989) and Reid (1993). Furthermore, these tubular structures can be plastically made to turn inside–out or outside–in, known as tube inversion. Finally, these structures can be made to split and curl up.

Most of the devices mentioned above are tested under quasi-static conditions of loading; at high strain rate, the flow stress of metals depends on the strain rate value (Johnson, 1972; Zaid and Harding, 1974). Hence, its effect in increasing the flow stress is included by using a simple scaling factor based on the mean strain rate in the loading process (Perrone, 1970). Moreover, the mode of deformation of the structure at high rate of strain may be significantly different from the quasi-static mode due to the inertia forces. In fact, the problems in structural plasticity cannot be easily resolved, due to many considerable factors: the effect of large geometry changes, hardening and strain rate effects, and the different modes of deformation governing the interaction between the above factors and the type of the employed material.

An examination of the relevant literature reveals that tubular structures are efficient in absorbing energy (per unit weight of the material used) in comparison with other structural elements. Generally, a desirable characteristic for these devices is a relatively constant crushing force. The comparison between the mechanical behavior of these elements under axial and lateral loads gives a number of different deformation mechanisms. In fact, on lateral loading conditions, the energy absorbed can be characterized by a smooth load–deflection relation, and these tubes are also easier to build than most other devices. Their efficiency is not affected by the load direction, whereas in the case of axial loading many disadvantages can be recorded, such as the large fluctuations of load about a mean value that is smaller than the initial peak load, and the extreme sensitivity to the load direction.

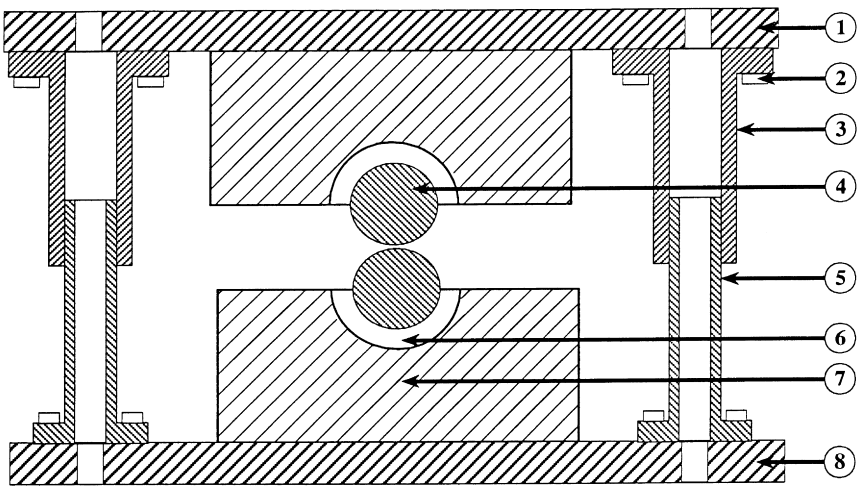

1: upper platen 2: screw 3: bush 4: specimen

5: guide 6: specimen accommodator 7: base 8: lower platen

Fig. 1. Sectioned view of the employed rig.

Table 1
Dimensions of tested cylinders

No.	(d_o), mm	(d_i), mm	$d_i/d_o(R)$	Length l_o, mm	Volume, mm^3
1	24.4	0.0	Solid	120	56,111.56
2	24.7	2.5	0.1	120	56,910.57
3	24.9	5.08	0.204	120	56,002.37
4	25.5	7.2	0.283	120	56,398.81
5	25.7	7.71	0.3	120	56,647.24
6	26.1	9.1	0.348	120	56,397.87
7	27.2	11.7	0.43	120	56,826.69
8	27.7	13.1	0.473	120	56,141.51

In the present work, to simulate the dynamic lateral collapse of an identical pair of specimens made from a classical engineering material, an experimental study is performed using solid and hollow (different geometries) specimens made from superplastic tin–lead alloy as a representative material due to its sensitivity to low strain rates. The deformation mechanism is appropriately determined employing plasticine colored specimens. A simple mathematical formulation is proposed to describe the mechanical behavior of identical hollow cylinders of inside/outside diameter (d_i/d_o) ratio, R, ranging from 0–0.473 compressed between two semi-cylindrical platens along their common tangent (Fig. 1) at different strain rates.

2. Experimental procedure

Cylindrical specimens, either solid or hollow, of different $d_i/d_o(R)$ values made from superplastic tin–lead (61.9–38.1% by weight) alloy were produced by forward extrusion with about 80% reduction. As all these different right circular specimens have almost the same cross-sectional area, hence, the initial billet size of 56 mm diameter is always used to produce these cylinders. The extruded specimen lengths are systematically of 120 mm. A length of 20 mm is always discarded from each end of cylinder after extrusion. All the hollow cylinders are produced using different bore of extrusion cylinders and different diameter mandrels. It is worth noting that, in the case of hollow cylinder production, the initial billets have to be drilled, before achieving the extrusion process, according to the mandrel's diameter value. The reduction ratio, in the solid case ($d_i/d_o = 0$), is of 81%, while in the second extremity case ($d_i/d_o = 0.473$), the reduction represents 80%. Thus, the maximum deviation cannot exceed 1% giving rise practically, as it is assumed, to the same material properties. The final dimensions of the employed cylinders are listed in Table 1. The experimental tests are carried out using a special rig, as shown in Fig. 1. This rig consists of a steel frame, which holds and locates two thick semi-cylindrical parts that accommodate and hold in position the cylinders to be tested. All the experimental tests are loaded between the platens of an Instron Universal Testing Machine at four constant cross head speeds, namely 0.2, 0.5, 2 and 10 mm/min, giving, respectively, average stabilized strain rates of 7×10^{-5}/s, 1.8×10^{-4}/s, 7×10^{-4}/s and 3.5×10^{-3}/s. In order to ensure the experimental results accuracy, each test was repeated twice under the same experimental conditions (applied speed and temperature). The tests are always conducted at room temperature (isothermal case). If the difference between the two responses exceed 3%, then another test has to be performed. For each case of R, four tests are conducted under increasing loading at different strain rates given above. Fig. 2(a–c) shows some selected load–deflection behaviors, as typical examples in the case of $R = 0.1$, 0.3 and 0.43. Experimentally, the energy absorbed at any corresponding deflection is estimated from the area under the load–deflection curve, using a planimeter, which determines the total energy absorbed.

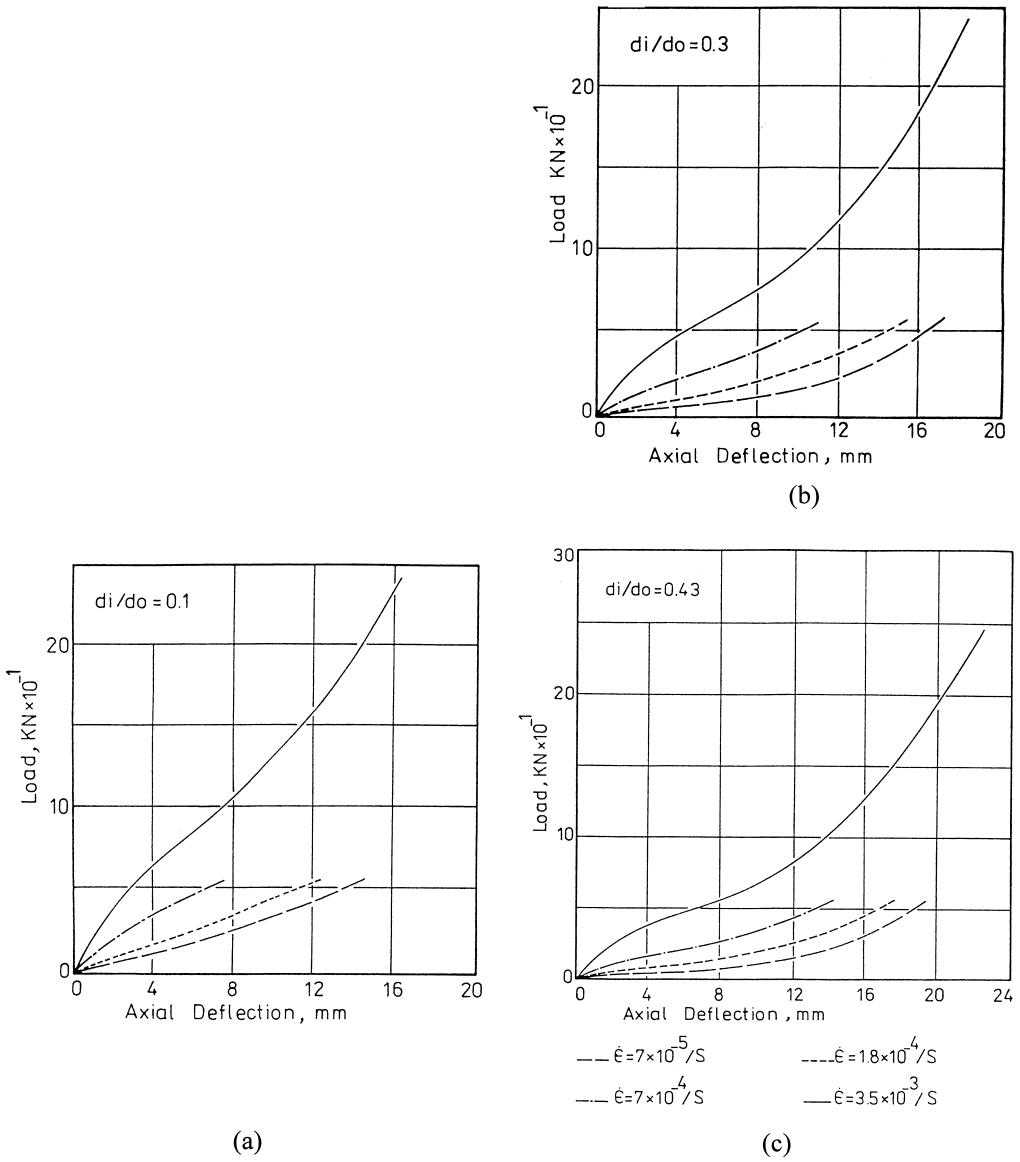

Fig. 2. Load–deflection curves at different strain rates for the specimens of: (a) $R = 0.1$; (b) $R = 0.3$; (c) $R = 0.43$.

3. Results and discussion

It is well known that most of the engineering metallic materials do not exhibit any changes under quasi-static loading conditions. But their strain rate sensitivity, for most of them, starts to be effective beyond the value of 1/s (Johnson, 1972). Thus, any change in strain rate in this range can induce a sensitivity, which makes the flow stress change in a similar manner to the superplastic tin–lead alloy. Consequently, this alloy can satisfactorily be used to simulate the metallic materials under dynamic strain rates. To realize this study under quasi-static loading condition, it becomes a relatively simple

task, and most of the experimental difficulties related to the dynamic loading situations can be overcome. However, it should be underlined that in many cases the mode of deformation under dynamic loading is different from that under quasi-static one, particularly when elastic and plastic stress wave effects dominate, or when thermoplastic phenomenon occurs (Johnson, 1972).

Let us now discuss the different experimental results carried out to determine the specimen geometry and the strain rate effects on the energy absorption for all mentioned cases (Table 1).

3.1. Load–deflection characteristic

Fig. 2(a–c) displays that whatever R and $\dot{\varepsilon}$ values, there are obviously three phases of force evolution during the plastic collapse; first, for a small axial deflection, the compressive force evolves rapidly with δ. Then, in the second phase, this evolution slows down for certain range of δ. This is due to the equilibrium between the increasing of the flattened area in the free deformation region of the two cylinders (outer cylinder halves, see Fig. 1) and the relative decreasing of the strain rate. Note that this free deformation region is called 'Tangential Region' (TR). Contrary to the second phase, the force evolves rapidly with δ in the third phase. In fact, this phenomenon can be interpreted by the fact that for a relatively high value of δ, the strain rate reaches practically its steady state, while the cylinders continue to be flattened in the TR, giving a large area of contact and hence high frictional stresses, to which the sudden change in force evolution is attributed. Whatever the value of R, this behavior is clearly observed at the highest strain rate (3.5×10^{-3}/s). It can be also noted from examination of Fig. 2(a–c) that the load–deflection curve plotted, at different strain rates, indicates that the required force increases whenever the strain rate is increased for a given deflection. The curves diverge with increasing deflection due to the change in the strain rate reflecting the material sensitivity to strain rate. In addition, it has been noticed that the deflection increases with an increase in the R ratio. For example, at a load of 50 kN, the deflections in the specimens of R of 0.1, 0.3 and 0.43 are, respectively, 2.9, 4.4 and 6.5 mm at an average strain rate of 3.5×10^{-3}/s, while the deflections of 13.6, 16.3 and 18.8 mm result at an average strain rate of 7×10^{-5}/s. In conclusion, at any particular load, the deformation increases as the R ratio is increased. Similarly, as the strain rate increases, the required load is also increased at any particular deflection.

3.2. Mechanism of deformation

A simple qualitative attempt is performed to determine the mode of deformation during plastic collapse. It is known that the plasticine, which is a non-metallic material, can represent the metallic materials behavior under high temperature and strain rate (Green, 1951; Rowe, 1977). Specimens of the same dimensions as those used in the experiments are made from different plasticine colors in order to study the deformation mechanism along the sides and length of the cylinders as well as around the cylinder bore. It is intriguing to note that the strain rate, axial deflection and specimen geometry are the main factors governing the plastic collapse mechanism. Consequently, three d_i/d_o ratios ($R = 0$, 0.283 and 0.473) are tested at different strain rates (10^{-5}/s, 10^{-4}/s and 10^{-3}/s) and axial deflections. The elastic response is negligible with respect to the plastic response. By increasing the lateral compressive loading, the initial linear contact transforms progressively to an area (flattening process). The greater the compressive force, the greater is the flattened area for a given strain rate and a specimen geometry.

An examination of Fig. 3 points out the deformed case of $d_i/d_o = 0$ for an axial deflection of $(\delta) =$ 15 mm at three different strain rates. During the compressive loading, the colored plasticine layers in the TR are flattened in the axial and width directions. In contrast, the two semi-cylindrical parts, constrained by the specimen accommodator, remain almost without plastic deformation effect (Fig. 3(a–c)). As can be seen from these figures, the upper part of the upper cylinder and the lower part of the

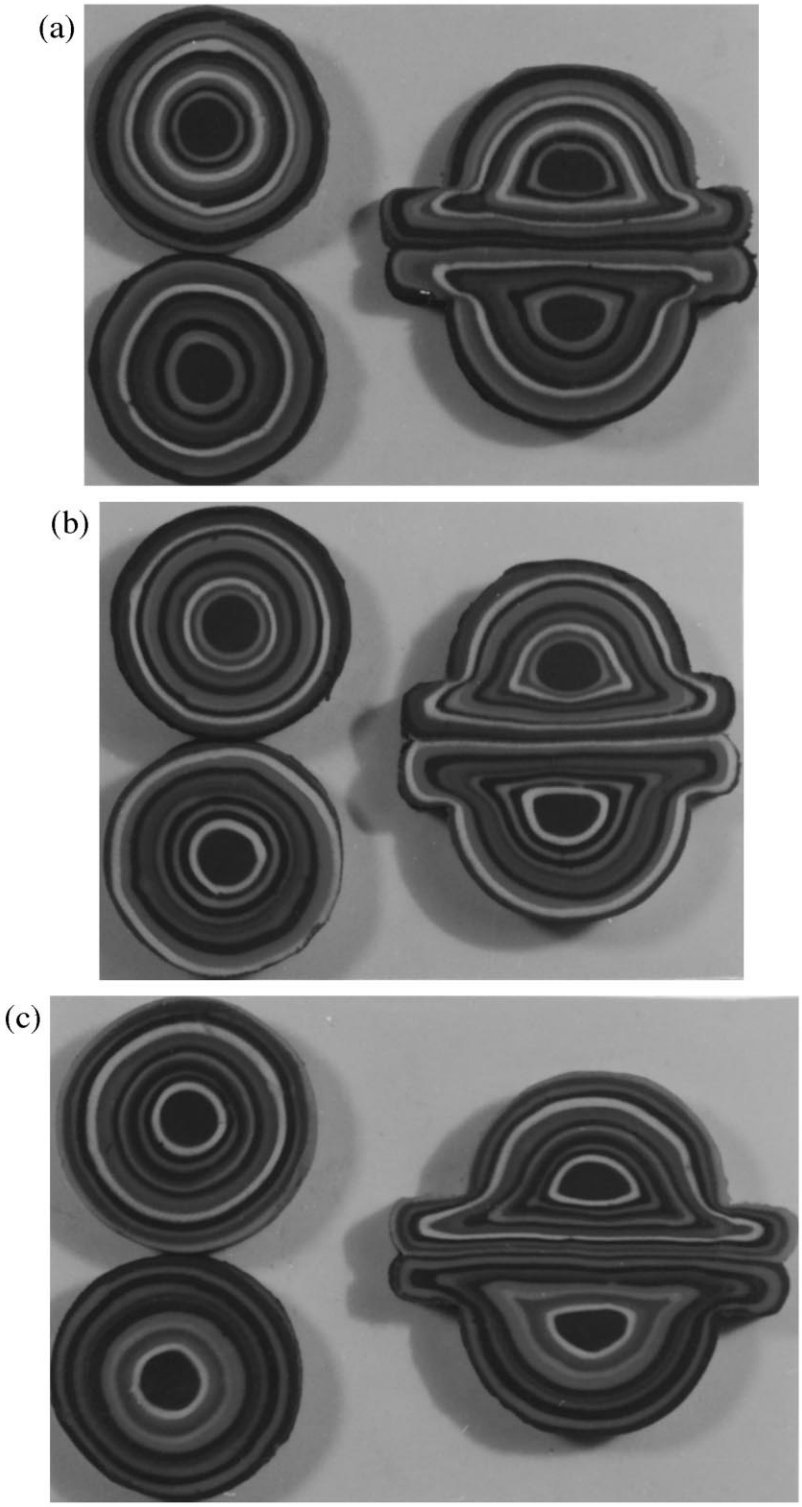

Fig. 3. Cross sections of plasticine colored specimens of $R = 0.0$ for $\delta = 15$ mm at (a) $\dot{\varepsilon} = 7 \times 10^{-5}$/s, (b) $\dot{\varepsilon} = 1.8 \times 10^{-3}$/s and (c) $\dot{\varepsilon} = 7 \times 10^{-3}$/s.

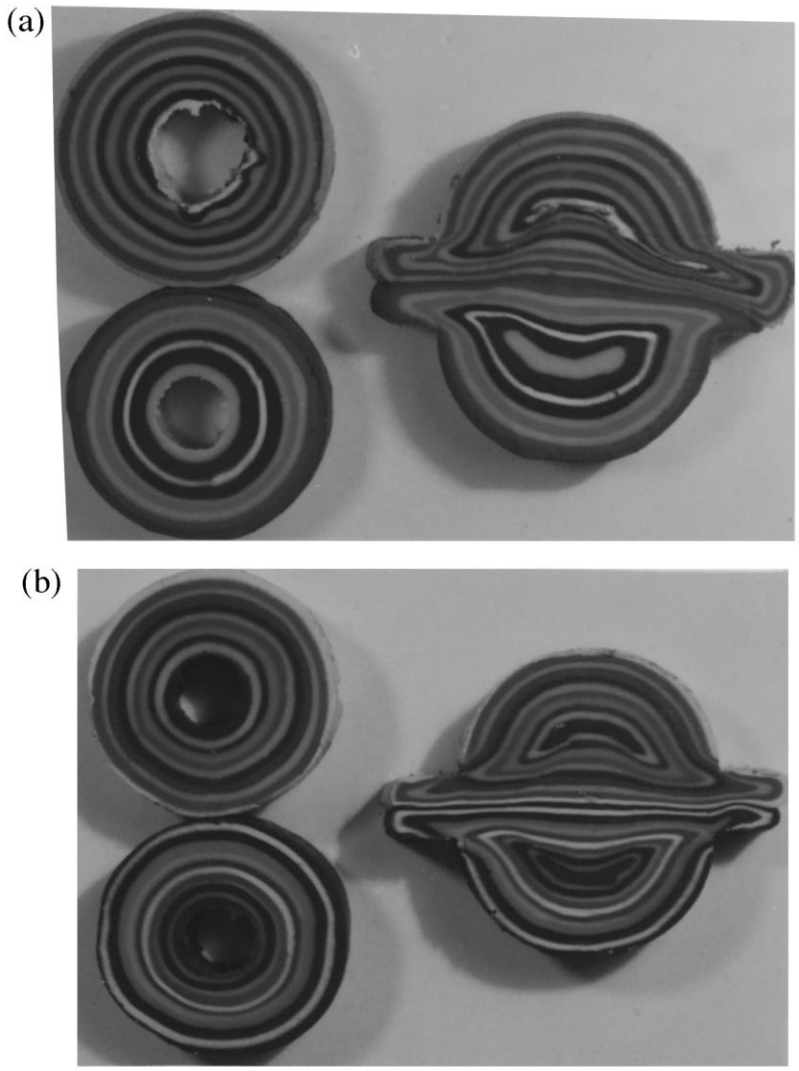

Fig. 4. Cross sections of plasticine colored specimens of $R = 0.283$ for $\delta = 20$ mm at (a) $\dot{\varepsilon} = 7 \times 10^{-5}$/s, (b) $\dot{\varepsilon} = 7 \times 10^{-3}$/s.

lower cylinder remain practically in their initial state. Whilst, the first observed external layer is torn (for each cylinder) along the length in the edged region of the two parts of the used rig. This is due to sharpness and constraining of plastic deformation, as well as to stress concentrations in this region. The successive deformed layers remain continuous in spite of their large deformations. This mechanism is always observed whatever the axial deflections and strain rates, and becomes more obvious under higher displacements and strain rates.

In the case of $R = 0.283$, the mechanism of plastic deformation is somewhat different from that in the solid specimen ($R = 0$). This is due to the existence of the cylinder bore, which has an influence on the deformation mechanism. Its influence depends strongly on its dimension, i.e., R value. Progressively, with the increasing of axial displacement, the colored layers of both specimens take a convex shape towards the bore. In fact, to fill up the bore, the flow mechanism occurs naturally in the bore direction, as shown in Fig. 4(a) and (b). It is clear that such mechanism is more important in the middle part of the TR than along the sides of two identical cylinders. Actually, when the material along the specimen sides is severely squeezed between the two parts of the used rig, the friction in this region becomes greater than the middle region especially in the relatively large displacement case. This provokes material flow towards the bore. Consequently, a wavy interface across the different colored layers takes place notably in this middle part. Based on experimental results, it is obvious that the bore closure definitively occurs first in the extremist bore sides before the middle part (Fig. 4(a)). In addition, the closure operation increases with the higher strain rate values at the same axial deflection.

For a relatively higher d_i/d_o ratio ($R = 0.473$), the mechanism of deformation is quite different from these previous cases ($R = 0$ and 0.283). This is due to the increasing of the cylinder bore dimension (a relatively important geometrical change). Note that for $R = 0$ and 0.283, the semi-cylindrical parts constrained by the specimen accommodator remain practically undeformed and the plastic deformation takes place mainly in the TR whatever the strain rate value is. Whereas, the $R = 0.473$ and $\delta < 22$ mm at average strain rate of $\dot{\varepsilon} = 1.8 \times 10^{-3}$/s, it is observed, for greater axial deflection (Fig. 5(a)) that the flow mechanism is taking place towards the bore direction (in the middle part of the contact zone). On the other hand, the experimental observations reveal that the strain rate plays an important role in the flow mechanism. Fig. 5(b) shows the complete bore closure state under the condition of $\delta = 25$ mm and $\dot{\varepsilon} = 7 \times 10^{-3}$/s. Moreover, it seems from examination of Fig. 5(b) that there is a flow mechanism in the semi-cylindrical constrained parts around the bore direction, i.e., change of deformation mechanism. According to an unpublished study already prepared by the author, this changing is taking place for $R \geqslant 0.43$ in comparison to the cases of $R \leqslant 0.4$, supporting the assumption adopted in this work. Furthermore, the amplitude of the wavy interface across the different colored layers in this middle part becomes more obvious for the nearest layers to the cylinder bore (Fig. 5(b)).

As a conclusion, the flow mechanism, especially around the bore, is influenced by the axial deflection, the applied strain rate and the specimen geometry. In addition, for a range of $0 \leqslant R \leqslant 0.348$, this mechanism is almost similar, while a change is experimentally recorded in the deformation mode for $R \geqslant 0.43$.

3.3. *Effect of strain rate and* R *ratio on the energy absorbed*

For different strain rates, the variation of the energy absorbed per unit volume vs the axial deflection is shown in Fig. 6. For such a system, it is clearly found that the energy absorbed per unit volume increases as the axial deflection and the strain rate increase. Generally, at any corresponding deflection and R ratio, we observe also that there is a sudden change in the amount of energy absorbed per unit volume as the strain rate is increased. This is based on the sensitivity of the used material to the change of strain rate, notably in the range of 10^{-4}/s–10^{-3}/s.

As far as the variation of the energy absorbed per unit volume with R is concerned, it is recorded for

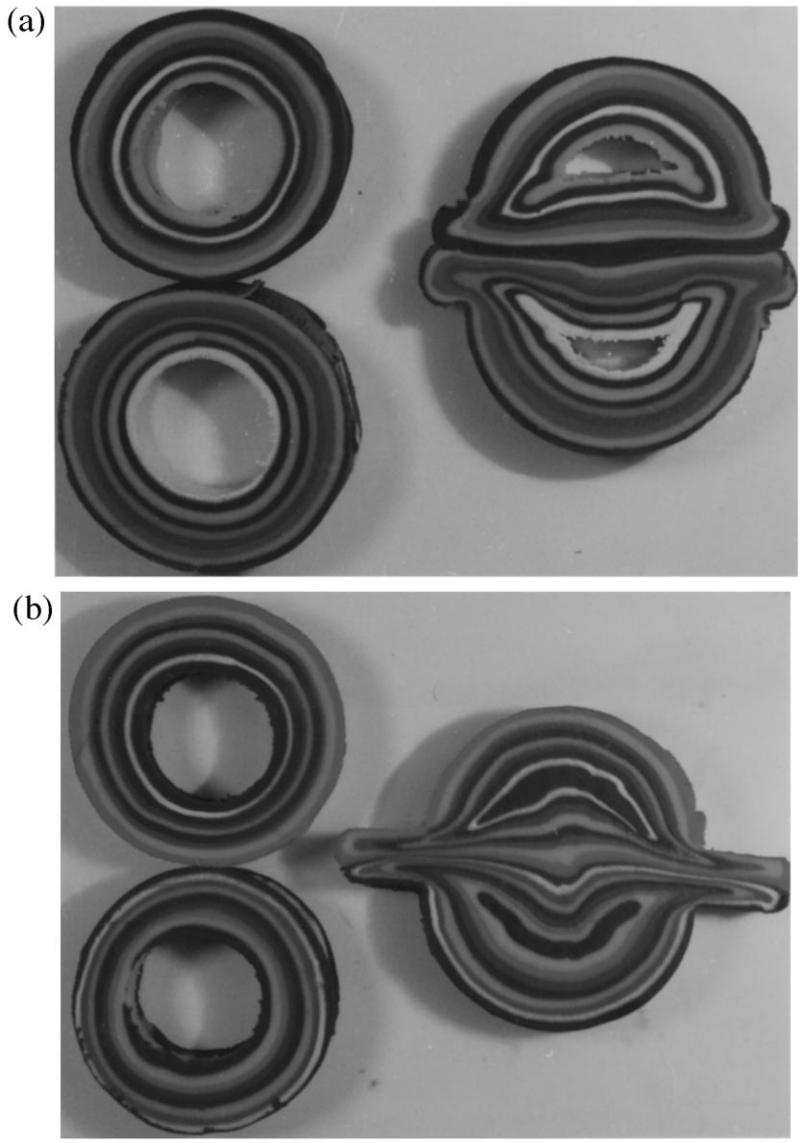

Fig. 5. Cross sections of plasticine colored specimens of $R = 0.473$ at (a) $\delta = 22$ mm and $\dot{\varepsilon} = 1.8 \times 10^{-3}$/s, (b) $\delta = 25$ mm and $\dot{\varepsilon} = 7 \times 10^{-3}$/s.

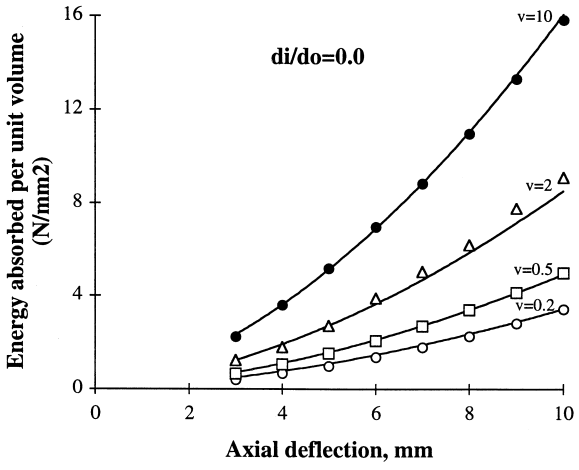

(a)

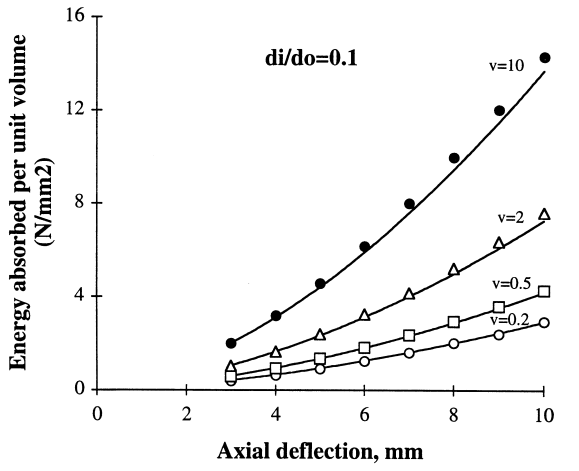

(b)

Fig. 6. Comparison between the experimental and theoretical variation of energy absorbed per unit volume and axial deflection at different strain rates for specimens of: (a) $R = 0.0$ (correlated results); (b) $R = 0.1$ (predicted results); (c) $R = 0.204$ (correlated results); (d) $R = 0.283$ (correlated results); (e) $R = 0.3$ (predicted results); (f) $R = 0.348$ (predicted results); (g) $R = 0.43$ (predicted results); and (h) $R = 0.473$ (correlated results).

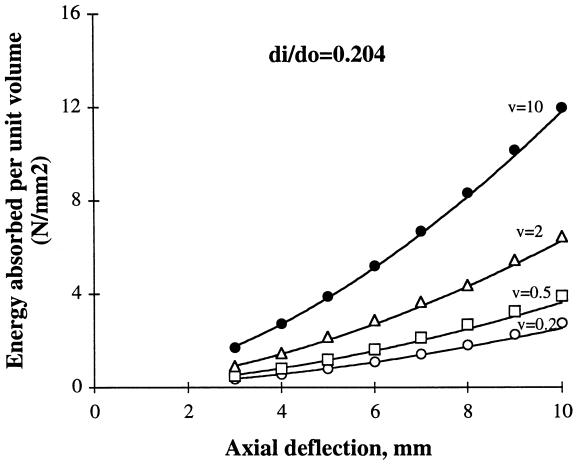

(c)

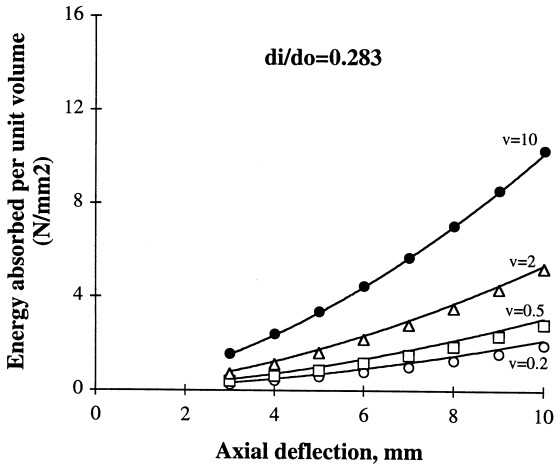

(d)

Fig. 6 (*continued*).

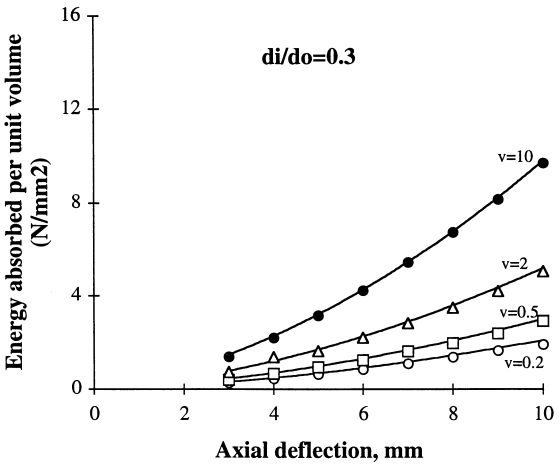

(e)

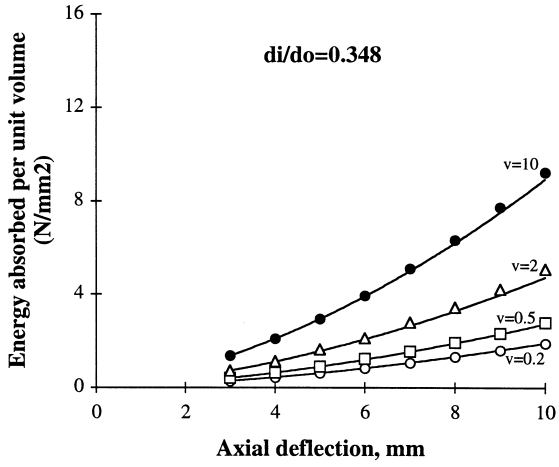

(f)

Fig. 6 (*continued*).

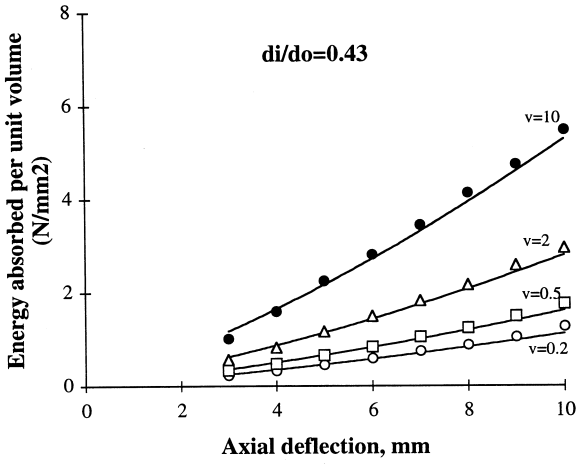

(g)

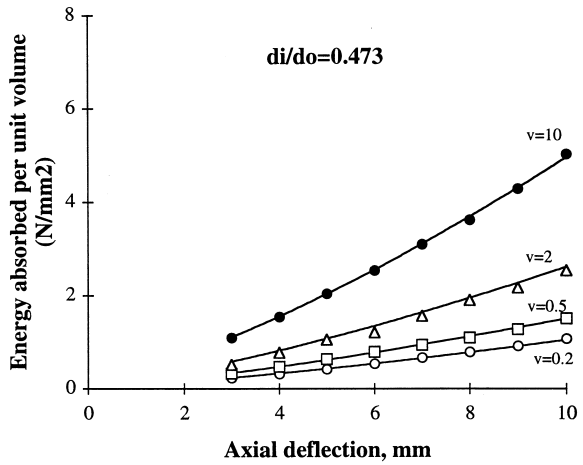

(h)

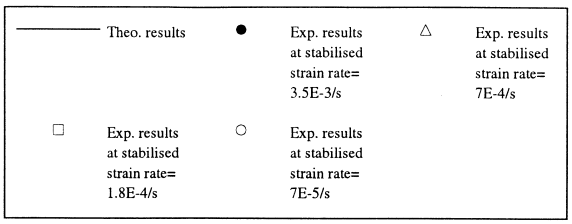

Fig. 6 (*continued*).

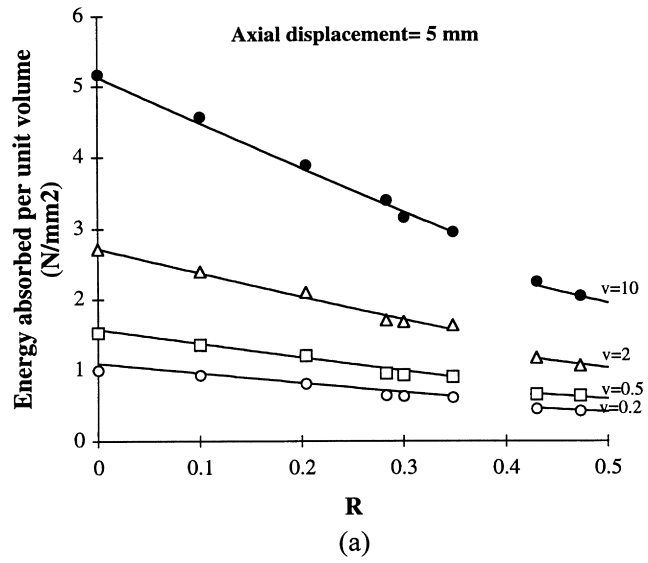

Fig. 7. Comparison between the experimental and theoretical effect of R on the energy absorbed per unit volume at different strain rates for axial deflection: (a) $\delta = 5$ mm; and (b) $\delta = 8$ mm.

two axial deflections of 5 and 8 mm (Fig. 7) for four strain rates. This shows that the factor R has a significant effect on the energy absorption for a given axial deflection and strain rate. Furthermore, these figures also point out that the relationship between the energy absorbed per unit volume and R ratio at strain rate of 7×10^{-5}/s and 1.8×10^{-4}/s is of a relatively similar pattern. However, this behavior starts to change at a strain rate of 7×10^{-4}/s, in which the effect of changing R on the absorbed energy is more steep, while at a strain rate of 3.5×10^{-3}/s the change becomes sharper, and this is due to the fact that the superplastic materials are more sensitive to strain rate at a range of 10^{-4}/s–10^{-3}/s. This is in agreement with previous results (Al-Naib and Duncan, 1970).

Finally, for this energy absorbing device, it might appear experimentally that the energy consumed during the plastic flow in the flattening of the two cylinders in the TR and in closure of the bore is more than that consumed along the length.

4. Formulation

Superplastic tin–lead alloy is used as a model material to simulate the dynamic lateral compressive behavior of rate sensitive metallic cylinders at high strain rate. From the energy dissipated viewpoint, a simple proposed mathematical formulation is devoted to describe the mechanical behavior of an identical pair of cylinders during their plastic collapse under dynamic loading. In this simple modeling, we take into consideration three principal parameters, which govern the energy absorption. These are the axial deflection, the strain rate and the specimen geometry.

The stress–strain characteristic of the employed superplastic alloy is determined using the same method reported by Al-Naib and Duncan (1970). The mechanical behavior can be simply expressed by the following equation:

$$\sigma = K\dot{\varepsilon}^n \tag{1}$$

where σ is the flow stress (N/mm^2), K represents a material constant and n is the strain rate sensitivity parameter.

Based on the experimental observation recorded above, it is found that, for a given specimen geometry, the total amount of energy absorbed (W^{T}) is proportionally related to the strain rate $\dot{\varepsilon}$ and to the axial deflection δ. This relation is assumed to be of non-linear type as shown in Fig. 6, thus:

$$W^{\mathrm{T}} = f(\dot{\varepsilon}^n, \delta^{\mu}) \tag{2}$$

It is now evident that the specimen geometry (R) plays an important role in the capacity of the system to absorb the energy (see Fig. 7). In order to take this factor into account, eqn (2) can be then written as

$$W^{\mathrm{T}} = \lambda\dot{\varepsilon}^n\delta^{\mu} \tag{3}$$

where λ and μ are parameters proposed to be functions in the geometrical ratio $R(d_{\mathrm{i}}/d_{\mathrm{o}})$ given by:

$$\lambda = f_1(R) \tag{4}$$

and

$$\mu = f_2(R) \tag{5}$$

A suitable and simple mathematical definition for each geometrical parameter is chosen. To define appropriately these functions in eqns (4) and (5), a simple linear relationship is proposed. Thus, we have

$$\lambda = \phi - \eta R \tag{6}$$

$$\mu = \phi_0 - \eta_0 R \tag{7}$$

where ϕ, ϕ_0, η, η_0 are constants related to the geometry factor.

As far as the representative strain rate estimation is concerned, the deformation mechanism is influenced, as shown above, by three main factors: the geometry of the cylinder, the axial deflection and the compressive speed (strain rate). This study gives an appropriate idea about the strain rate evaluation. In fact, under a constant lateral compressive loading, the strain rate evolves locally in the TR when the axial deflection has a very small value giving rise to a relatively considerable strain rate value (the first phase of force evolution during the plastic collapse). In other words, the greater the axial displacement, the greater the flattening process that takes place, the lower becomes the strain rate. Hence, it is assumed that its value continues to gradually decrease with increasing the axial deflection up to a stabilized value in spite of a constant compressive speed application. For such complicated structures, the strain rate evaluation represents a hard task. In addition, its estimation seems to be more realistic in the case of finite element analysis.

When the axial deflection has a relatively large value, the deformation mode becomes, as shown above, more complex due to the triaxiality of the plastic flow. Therefore, precise strain rate determination is not a simple analysis especially in the case of hollow cylinder structures having a considerable value of R ($R < 0.4$). This means that the flow mechanism becomes extremely complex due to the existence of the cylinder bore. The main objective of this part is to propose a simple model describing the mechanical behavior of the used structure during its plastic collapse. For this reason, simplified and approximated mathematical evaluation of the representative strain rate is chosen for such simple modeling. Note that all representative strain rate values given here correspond to stabilized values. Its mathematical definition is expressed as follows:

According to Calladine and English (1984), the mathematical definition of the average strain rate is given by

$$\dot{\varepsilon} = Cv \tag{8}$$

where C is a constant and v is the compressive speed (mm/s). The representative strain rate evaluation is based here on the above equation. In fact, some mathematical modifications are made in (8) to adapt it for the actual used structure. For the employed system, the strain rate has a considerable value especially for considerable small deflections. Gradually, its value decreases with the increasing of δ, until it reaches, as it is assumed, the steady state as illustrated in Fig. 8. In order to describe reasonably its evolution, the constant C is proposed to be a function of axial deflection δ given by this relation:

$$C = 1/h \tag{9a}$$

and

$$h = \beta(1 - \mathrm{e}^{-\delta\alpha/2}) \quad \text{with } (\delta > 0) \tag{9b}$$

where β represents the asymptotic value of h and α being a parameter which controls the speed of saturation of β. Note that the second term in the right-hand side of eqn (9b) will be reduced as $\delta/2$ increases (for each cylinder), giving consequently $h = \beta$ (at stabilization). In this case, the initial definition of the strain rate of Calladine and English (1984) can be retrieved [eqn (8)]. As pointed out above, the plastic deformation is affected by the structural geometry of the specimens (value of R), thus the corresponding representative strain rate is naturally affected by this factor. However, in this framework, for the sake of simplicity, a unified definition of the strain rate is proposed for all different

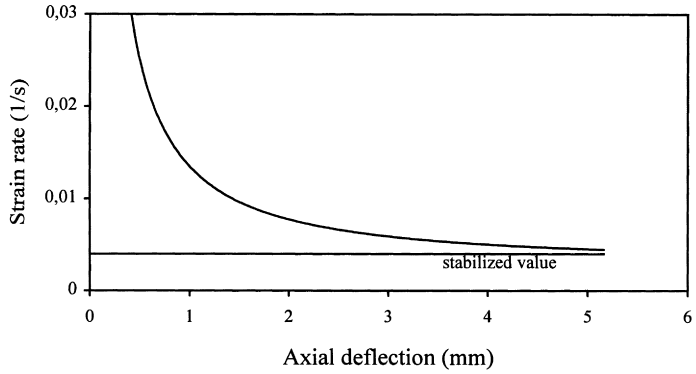

Fig. 8. A plot of predicted average strain rate evolution during the plastic collapse.

cases of R. In reality, the exact strain rate evolution and its estimation are extremely complex whatever the cylinder geometry is. Simplified and approximated solution is thus adopted for describing its average evolution. Therefore, the representative strain rate is expressed by

$$\dot{\varepsilon} = v/\beta(1 - e^{-\delta\alpha/2}) \tag{10}$$

The total amount of energy absorbed can be deduced by substituting eqns (6) and (7) in eqns (3) as follows:

$$W^{T} = (\phi - \eta R)\delta^{(\phi_0 - \eta_0 R)}\dot{\varepsilon}^{n} \tag{11}$$

W^{T} is in Joule.

The energy absorbed per unit volume (W^{V}) can be determined by:

$$W^{V} = W^{T}/v_0 \tag{12a}$$

$$W^{V} = \left[(\phi - \eta R)\delta^{(\phi_0 - \eta_0 R)}\dot{\varepsilon}^{n}\right]/v_0 \tag{12b}$$

where W^{V} is in N/mm^2, $v_0 = (\pi l_0/4)(d_o^2 - d_i^2)$ is the volume of the specimen and l_0 represents the initial length of the specimen.

4.1. Identification of the model parameters

The main goal of this section is to determine quantitatively those parameters used in the proposed model. For this process, the experimental results of $R = 0$, 0.204, 0.283 and 0.473 are used as experimental data bases for determining these parameters. The experimental results of $R = 0.1$, 0.3, 0.348 and 0.43 are used as data bases for the validation process of calibrated parameters.

The experimental investigation of the flow mechanism presented in the previous paragraph demonstrates that, for a studied range of R ($0 \leqslant R \leqslant 0.473$), a change in the flow mechanism is observed. The mechanical behavior (related notably to the energy absorbed) of the employed system is consequently influenced by this change. It is almost certain that the plastic strain of cylinders in the range of $0 \leqslant R \leqslant 0.348$ is governed by flow mechanisms more or less similar. In the light of these results and whatever the strain rate is, the mathematical definition of the mechanical behavior (energy absorbed) is described by eqns (11) and (12) possessing the same material constants concerning this

geometric range ($0 \leqslant R \leqslant 0.348$). On the other hand, for $R \geqslant 0.43$ and whatever the strain rate is, another flow mechanism is observed. Therefore, the coefficients related to the geometry effect (ϕ, ϕ_0, η and η_0) have to be different from the coefficients determined according to the first range. Note that, for all different used cylinders, the coefficients related to the material properties (K and n) and those of strain rate estimation (β and α) remain without modification. Two sets of identified parameters, which can appropriately describe the mechanical behavior of the cylinders, are given in Table 2.

First of all, to determine the two parameters of the mechanical behavior of superplastic alloy (K and n), a small circular billet is tested under simple compression load at different strain rates. The overall closeness between the experimental and theoretical results, which provided a good general fit, can be obtained (Table 2). Generally, six parameters (ϕ, ϕ_0, η, η_0, β and α) need identification. So, the proposed model is programmed into a small computer code as a tool to solve the identification problem using an appropriate experimental data base. The identification process is generally a hard task especially in the case of non-linear material behavior. However, with a simple explicit proposed model, this process can be carried out in a simple manner. The computer code used to calibrate all model parameters is based on the resolution technique of the non-linear optimization problem. In fact, gradient algorithm (iterative method) (Minoux, 1983) is employed to obtain these parameters. In order to satisfactorily carry out this operation the following procedures are adopted:

(a) Identification of the coefficients related to the first geometry range ($0 \leqslant R \leqslant 0.348$): the initial values of the parameters are chosen based on the experimental results ($R = 0$, 0.204 and 0.283). Then, by performing several iterations, the best results are obtained when the deviation between the experimental and theoretical results becomes minimal. In other words, these parameters are specified by having the best fit between the theoretical and experimental results. The obtained results are shown in Table 2. During this operation, the values of β (asymptotic value) and α which are already defined related to this range, should be valid for the second geometric range. This choice is compatible with the assumption adopted above for strain rate estimation. These calibrated values give the representative conventional strain rates corresponding to the employed cross head speeds.

(b) To correlate the second geometric range (for $R \geqslant 0.43$), the geometrical parameters (ϕ, ϕ_0, η, η_0) must be recalibrated. This task is achieved by using the experimental data of $R = 0.473$. It is interesting to note that this step should be performed by fixing all the identified parameters concerning the mechanical behavior of superplastic alloy (K and n) and the strain rate estimation (β and α). The suitable defined parameters, for this range, are given in Table 2. After this process, we find that the correlated solutions are effectively in good agreement with the experimental results (see Fig. 6(a), (c), (d) and (h)). This is not surprising, since we have used these results for calibrating the model parameters that can describe the energy dissipated during the plastic collapse of the system.

Table 2
Identified parameters of the model

Parameters	$0 \leqslant R \leqslant 0.348$	$0.43 \leqslant R \leqslant 0.473$
K	180	180
n	0.395	0.395
β	47.16	47.16
α	0.611	0.611
ϕ	143.0	167.5
η	157.4	136.3
ϕ_0	1.76	1.5
η_0	0.125	0.230

4.2. Validation

As for validation, simulation tests are performed by using the proposed model for characterizing the energy absorbed during the plastic strain of the cylinders. Therefore, the mechanical behavior of three R ratios (0.1, 0.3 and 0.384) is simulated using the first set of parameters, and $R = 0.43$ for the second set. Fig. 6(b), (e–g) represents the experimental evolution of the energy absorbed per unit volume vs the axial deflection compared with the predicted solution. It is clear that the proposed model is able to well describe the plastic collapse of an identical pair of cylinders under different strain rates and R ratios.

5. Conclusion

The superplastic tin–lead alloy can be used at a strain rate ranging from 10^{-4}/s–10^{-3}/s to represent the behavior of metallic materials in the intermediate and high strain rates 1/s–10^{4}/s.

The capability of the system to absorb the energy is increased by increasing the strain rate and decreasing the ratio R for the same volume and cross-sectional area. Under the same load and strain rate, the amount of deflection in the specimen decreases with the decrease in the R ratio.

Colored plasticine specimens are successfully used in order to understand and to determine the flow mechanism and the mode of deformation during the lateral mechanical collapse of an identical pair of cylinders.

The proposed formulation can successfully describe the plastic collapse of an identical pair of cylinders under different strain rates and R ratios.

References

Abramowicz, W., Jones, N., 1986. Dynamic progressive buckling of circular and square tubes. Int. J. Impact Engng 4, 243–270.

Al-Naib, T.Y.M., Duncan, J.L., 1970. Superplastic metal forming. Int. J. Mech. Sci. 12, 463–477.

Calladine, C.R., English, R.W., 1984. Strain-rate and inertia effects in the collapse of two types of energy-absorbing structure. Int. J. Mech. Sci. 26, 689–701.

Ezra, A.A., Fay, R.J., 1972. An assessment of energy absorbing devices for prospective use in aircraft impact situations. In: Hermann, G., Perrone, N. (Eds.), Dynamic Response of Structures.

Green, A.P., 1951. The use of plasticine models to simulate the plastic flow of metals. Phil. Mag. Ser. 7, 42, 365–373.

Johnson, W., 1972. Impact Strength of Materials. Edward Arnold, London.

Johnson, W., Reid, S.R., 1978. Metallic energy dissipating systems. Appl. Mech. Rev. 31, 277–288.

Johnson, W., Reid, S.R., 1986. Update to "Metallic energy dissipating systems". Appl. Mech. Rev. 31, 277–288 (1978); Appl. Mech. Update 1986, pp. 315–319.

Jones, N., 1989. Structural Impact. Cambridge University Press, Cambridge, UK.

Minoux, M., 1983. Programmation Mathématique. Dunod, Paris, France.

Perrone, N., 1970. Crashworthiness and biomechanics of vehicle impact. In: Dynamic Response of Biomechanical Systems, Proc. Winter Annual Meeting. ASME.

Rawlings, B., 1974. Response of structures to dynamic loads. In: Proc. Conf. on Mechanical Properties of Materials at High Rates of Strain. Institute of Physics, 279–298.

Reid, S.R., 1993. Plastic deformation mechanisms in axially compressed metal tubes used as impact energy absorbers. Int. J. Mech. Sci. 35, 1035–1052.

Rowe, W.G., 1977. Principle of Industrial Metal Working Processes. Edward Arnold, p. 22.

Zaid, A.I.O., Harding, J., 1974. Strain Rate Effects in 1.5%CrMo Steel, University of Oxford.